# Complexation of Polyaromatics by $C_5H_5Fe^+$ and $C_5Me_5Fe^+$ and Electronic Structures of the Monoreduced Complexes

Marc Lacoste,[†] Hassan Rabaa,[‡] Didier Astruc,*[,†] Albert Le Beuze,[‡] Jean-Yves Saillard,*[,‡] Gilles Précigoux,[§] Christian Courseille,[§] Nicole Ardoin,[†] and Walter Bowyer[†]

*Laboratoire de Chimie Organique et Organométallique, U.A. CNRS No. 35, Université de Bordeaux I, 351, Cours de la Libération, 33405 Talence Cédex, France, Laboratoire de Chimie du Solide et Inorganique Moléculaire, Université de Rennes I, Campus Beaulieu, 35042 Rennes Cédex, France, and Laboratoire de Cristallographie, Université de Bordeaux I, 351, Cours de la Libération, 33405 Talence Cédex, France*

*Received October 7, 1988*

The synthesis of a number of known complexes $[FeCp(\eta^6\text{-polyaromatic})]^+PF_6^-$ has been reproduced or improved in order to examine their cathodic and $LiAlH_4$ reduction to $Fe^I$ or the monoreduced state. It is found that the phenanthrene and pyrene complexes are not hydrogenated during the ligand exchange reaction with ferrocene and $AlCl_3$ and that pyrene does not give binuclear complexes, contrary to previous reports. The new complexes of triphenylene and of perylene have been made, and, although the latter is extremely light-sensitive, its X-ray crystal structure has been determined. It contains two different molecules in the unit cell where the two possibilities of relative conformations of the $C_5$ ring/$C_6$ ring are found. With $FeCp^*(CO)_2Br + AlCl_3$, the new complexes $[FeCp^*(\eta^6\text{-polyaromatic})]^+PF_6^-$ ($Cp^* = \eta^5\text{-}C_5Me_5$) have been made with biphenyl, phenanthrene, dihydrophenanthrene, triphenylene, and pyrene. Syntheses in the melt are suitable for both Cp and Cp* series. The first cathodic wave is chemically reversible only for polyaromatics with less than four fused rings in the Cp series, but, with Cp*, the reduction of the pyrene complex becomes reversible. The comparison of the thermodynamic redox potentials corresponding to the system $FeCp(polyAr)^{+/0}$ with those of the free ligand system $(polyAr)^{0/-}$ provides, according to Vlček's theory, the spin density on the polyaromatic ligand of the monoreduced complexes. Values are found to depend markedly on the number $n$ of fused rings of the polyaromatic in the Cp series so that significant spin density remains on Fe if $n \leq 4$, whereas it is mainly located on the polyaromatic if $n > 4$. This is not the case in the Cp* series where the Fe(I) state is stabilized, with residual spin density on the polyaromatic being about 15–30%. In order to understand the electronic structure of those compounds, calculations using both the EH and MS-SCF-X$\alpha$ formalisms have been performed on a series of complexes. The results concerning the spin densities are in reasonable (EH) or good (X$\alpha$) agreement with the experimental ones. However, the EH calculations on [FeCp(naphthalene)] lead to wrong results due to a poor level ordering of two a′ levels situated in the HOMO/LUMO region. All of the cationic $Fe^{II}$ complexes react with $LiAlH_4$ in THF at low temperature to give the neutral electron-transfer products. The ESR spectra of the latter also show a $d^7$ $Fe^I$ state for $n \leq 4$ (three $g$ values around 2) and a single line attributed to the radical anionic ligand if $n > 4$.

## Introduction

There is an increasing interest in the use of polyaromatics as molecular materials.[1-5] For instance, derivatives of triphenylene are used as discotic liquid crystals,[3] perylene can be doped with oxidants to provide organic conductors,[4,5] and several fused polyaromatics are fluorescent and luminescent agents and are used as photochromics.[1] The $\pi$ complexation of polyaromatics by a transition metal brings about a tridimensionality which should have a dramatic influence on the physical properties and could open new synthetic routes. As compared to simple arene complexes, fused polyaromatic complexes can have a weaker arene–metal bond, which is useful in catalysis or for any purpose requiring free coordination sites. A number[6] of chromium tricarbonyl complexes of polyaromatics are known, and $Cr(\eta^6\text{-naphthalene})(CO)_3$ was shown by Caïs to be a catalyst for the hydrogenation of dienes.[7] In the $FeCp^+$ series, the situation is confusing. Several publications have reported studies[8-15] of what were believed to be complexes of fused polyaromatics; in fact, it was shown later that these complexes are hydrogenated during their complexation with $FeCp_2 + AlCl_3 + Al$ (naphthalene, anthracene, phenanthrene, pyrene). Some true complexes are known, however (naphthalene, coronene,[14a] cyclophanes[14b-d]), but we have reinvestigated the synthetic problem. We were also interested in knowing

[†] Laboratoire de Chimie Organique et Organométallique, Université de Bordeaux I.

[‡] Laboratoire de Chimie du Solide et Inorganique Moléculaire, Université de Rennes I.

[§] Laboratoire de Cristallographie, Université de Bordeaux I.

(1) Ewald, M.; Lamotte, M.; Garrigues, P.; Rima, J.; Veyres, A.; Lapouyade, R.; Bourgeois, G. *Adv. Org. Geochem.* **1983**, 705.

(2) (a) Donn, B. *Astrophys. J.* **1968**, *152*, L129. (b) Basile, B.; Middeditch, B.; Oro, J. *Org. Geochem.* **1983**, *5*, 211.

(3) (a) Clar, E. *Polycyclic Hydrocarbons*; Academic Press: New York, 1964; Vols. 1 and 2. (b) Destrade, C.; Gasparoux, H.; Foucher, P.; Nguyeyn Hun Tinh; Malthete, J.; Jacques, J. *J. Chim. Phys. Biol.* **1983**, *80*, 137. (c) Levelut, A. M. *Ibid.* **1983**, *80*, 149.

(4) Dias, J. R. *Acc. Chem. Res.* **1985**, *18*, 241.

(5) Clar, E. *The Aromatic Sextet*; Wiley: London, 1972.

(6) (a) Kirss, R. V.; Treichel, P. M. *J. Am. Chem. Soc.* **1986**, *108*, 853. (b) Rogers, R. D.; Atwood, J. L.; Albright, T. A.; Lee, W. A.; Rausch, M. D. *Organometallics* **1984**, *3*, 263.

(7) Caïs, M.; Fraenkel, D.; Weidenbaum, K. *Coord. Chem. Rev.* **1975**, *16*, 27.

(8) Nesmeyanov, A. N.; Vol'kenau, N. A.; Bolesova, I. N. *Dokl. Akad. Nauk SSSR*, **1966**, *166*, 607.

(9) Nesmeyanov, A. N.; Denisovitch, L. I.; Gubin, S. P.; Vol'kenau, N. A.; Sirotkina, F. I.; Bolesova, I. N. *J. Organomet. Chem.* **1969**, *20*, 169.

(10) (a) Morrison, W. H., Jr.; Ho, E. Y.; Hendrickson, D. N. *J. Am. Chem. Soc.* **1974**, *96*, 3603. (b) Morrison, W. H., Jr.; Ho, E. Y.; Hendrickson, D. N. *Inorg. Chem.* **1975**, *14*, 500.

(11) Lee, C. C.; Demchuk, K. J.; Pannekoek, W. J.; Sutherland, R. G. *J. Organomet. Chem.* **1978**, *162*, 253.

(12) Lee, C. C.; Demchuk, K. J.; Sutherland, R. G. *Can. J. Chem.* **1979**, *57*, 933.

(13) Sutherland, R. G.; Pannekoek, W. J.; Lee, C. C. *Ann. N.Y. Acad. Sci.* **1977**, *295*, 192.

(14) (a) Gibb, T. C. *J. Phys. C* **1976**, *9*, 2627. (b) Koray, A. R. *Ibid.* **1981**, *212*, 233; **1982**, *232*, 345. (c) Swann, R. T.; Boekelheide, V. *Ibid.* **1982**, *231*, 143. (d) Laganis, E. D.; Finke, R. G.; Boekelheide, V. *Proc. Natl. Acad. Sci. U.S.A.* **1981**, *78*, 2657.

(15) Lacoste, M.; Astruc, D. *J. Chem. Soc., Chem. Commun.* **1987**, 667.

0276-7333/89/2308-2233$01.50/0 

**Chart I**

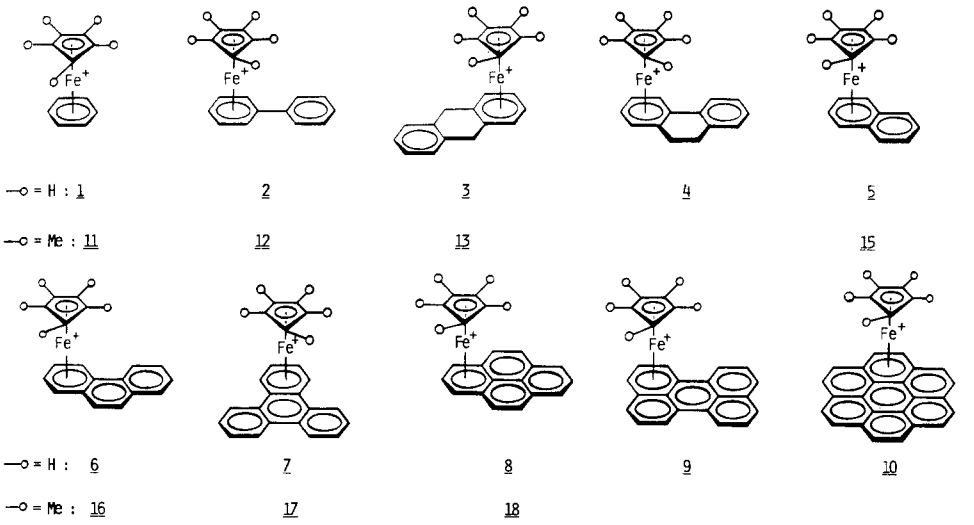


if new complexes of polyaromatics such as those of triphenylene and perylene could be made.

Thus, we have addressed the question of the complexation of $[(\eta^5\text{-}C_5Me_5)Fe]^+$ to fused polyaromatics. Next, we were concerned with the electroreduction of the cationic iron complexes by comparison with analogous complexes of simple arenes. In particular, we wished to know how the stability of the monoreduced state depends on the fused aromatic structure, what the distribution of spin density on the polyaromatic is, and if there is a correlation between these two factors. This latter aspect has been dealt with in a preliminary communication.[15] There is a large body of information[9,10b,15-22] concerned with the electroreduction of simple $[Fe^{II}Cp(arene)]^+$ complexes (two reversible one-electron waves), but there are few such reports on polyaromatic complexes although the recent work by Geiger et al.[20] on (cyclophane)iron complexes is most relevant.

## Results and Discussion

**I. Syntheses. (a) Complexation by $[FeCp]^+$.** The reactions proceed by ligand exchange between a Cp ring of ferrocene and the polyaromatic in the presence of $AlCl_3$ and Al;[8] water is avoided contrary to the complexation of simple arenes.[23,24] This type of reaction, first carried out by Nesmeyanov et al.,[25] was also done by the Russian group with naphthalene.[8]

$$FeCp_2 + \text{polyaromatic} \xrightarrow[Al]{AlCl_3} [FeCp(\eta^6\text{-polyaromatic})]^+ \quad (1)$$

Complexes of biphenyl,[8] phenanthrene,[11] pyrene,[10a,11,12] and coronene[26] are also known, and these syntheses have been reproduced here. However, it was reported that phenanthrene[11] and pyrene[12] are hydrogenated in the course of the ligand-exchange reactions. We have tried to repeat these reactions under various reaction conditions (change of temperature between 70 and 200 °C, amount and quality of $AlCl_3$, amount of Al powder) and were never able to find any hydrogenation product for these two aromatics. Only the non-hydrogenated complexes were obtained. Hydrogenated bimetallic complexes were also reported which we never found. The non-hydrogenated bimetallic phenanthrene complex was obtained and its electrochemistry will be discussed in a subsequent paper, but no bimetallic complex of pyrene was found by us, regardless of the reaction conditions. Coronene is not subjected to hydrogenation upon complexation. The new complexes of perylene and triphenylene were also made. Both were found as non-hydrogenated complexes, and the triphenylene complex is not hydrogenated even if the conditions are severe (excess $AlCl_3$, 200 °C). On the other hand, the case of perylene was not investigated at high temperature where it is probable that hydrogenation occurs as for naphthalene.[27] We also found that it is not necessary to use a solvent and the reactions proceed as well in the melt at 110–140 °C; this does not influence the possibility of hydrogenation, however. It significantly improves the yields of reactions. For instance, in the case of pyrene, the reaction yield (30%) is more than doubled.

**(b) Complexation by $[C_5Me_5Fe]^+$.** For this purpose, we used the technique that we first reported for the complexation of benzene and hexamethylbenzene.[28] The bromo complex $Fe(\eta^5\text{-}C_5Me_5)(CO)_2Br$ is used in the presence of $AlCl_3$ (no Al).

$$[Fe(\eta^5\text{-}C_5Me_5)(CO)_2Br] + \text{polyAr} \xrightarrow{AlCl_3} [Fe(\eta^5\text{-}C_5Me_5)(\eta^6\text{-polyAr})]^+ \quad (2)$$

Again, the solvent is useless and decreases reaction yields. It is unnecessary to use an autoclave. The new complexes of biphenyl, phenanthrene, triphenylene, and pyrene were synthesized (Chart I). The hydrogenation

(16) Dessy, R. E.; Stary, F. E.; King, R. B.; Waldrop, M. *J. Am. Chem. Soc.* **1966**, *88*, 471.
(17) (a) Astruc, D.; Dabard, R.; Laviron, E. *C.R. Acad. Sci., Ser. C* **1969**, *269*, 608. (b) Astruc, D.; Dabard, R. *Bull. Soc. Chim. Fr.* **1976**, 228.
(18) (a) Moinet, C.; Román, E.; Astruc, D. *J. Organomet. Chem.* **1977**, *128*, C45. (b) Moinet, C.; Román, E.; Astruc, D. *J. Electroanal. Chem.* **1981**, *121*, 241.
(19) (a) El Murr, N. *J. Chem. Soc., Chem. Commun.* **1981**, 219. (b) El Murr, N. *J. Chem. Soc., Chem. Commun.* **1981**, 251.
(20) Bowyer, W. J.; Geiger, W. E. *Organometallics* **1984**, *3*, 1979.
(21) Connelly, N. G.; Geiger, W. E. *Adv. Organomet. Chem.* **1984**, *23*, 1.
(22) Buet, A. Thesis, Rennes, 1980.
(23) Nesmeyanov, A. N.; Vol'kenau, N. A.; Petrakova, V. A. *Izv. Akad. Nauk SSSR, Ser. Khim.* **1974**, *9*, 2159.
(24) Astruc, D. Tetrahedron Report No. 157. *Tetrahedron*, **1983**, *39*, 4027.
(25) (a) Nesmeyanov, A. N. *Int. Union Pure Appl. Chem.* **1963**, 221. (b) Nesmeyanov, A. N. *Adv. Organomet. Chem.* **1972**, *10*, 1.
(26) Schmitt, G.; Keim, W.; Fleischhauer, J.; Walbergs, U. *J. Organomet. Chem.* **1978**, *152*, 315.
(27) Sutherland, R. G.; Chen, S. C.; Pannekoek, W. J.; Lee, C. C. *J. Organomet. Chem.* **1975**, *101*, 221.
(28) (a) Astruc, D.; Hamon, J. R.; Althoff, G.; Román, E.; Batail, P.; Michaud, P.; Mariot, J. P.; Varret, F.; Cozak, D. *J. Am. Chem. Soc.* **1979**, *101*, 5445. (b) Hamon, J. R.; Astruc, D.; Michaud, P. *J. Am. Chem. Soc.* **1981**, *103*, 758. (c) Michaud, P.; Astruc, D.; Ammeter, J. H. *J. Am. Chem. Soc.* **1982**, *104*, 3755. (d) Astruc, D. *Acc. Chem. Res.* **1986**, *19*, 377.

**Table I. Selected Bond Distances (Å) and Angles (deg) for [FeCp(perylene)]$^+PF_6^-$**

| molecule 1 | | molecule 2 | | molecule 1 | | molecule 2 | |
|---|---|---|---|---|---|---|---|
| (a) Within the Metal Coordination Sphere | | | | | | | |
| Fe(30)–C(1) | 2.16 (3) | Fe(90)–C(51) | 2.11 (3) | Fe(30)–C(31) | 2.07 (4) | Fe(90)–C(91) | 2.08 (3) |
| Fe(30)–C(6) | 2.10 (3) | Fe(90)–C(56) | 2.16 (3) | Fe(30)–C(32) | 2.04 (3) | Fe(90)–C(92) | 1.98 (4) |
| Fe(30)–C(7) | 2.15 (3) | Fe(90)–C(57) | 2.12 (3) | Fe(30)–C(33) | 1.96 (3) | Fe(90)–C(93) | 2.00 (4) |
| Fe(30)–C(8) | 2.15 (3) | Fe(90)–C(58) | 2.06 (3) | Fe(30)–C(34) | 2.06 (3) | Fe(90)–C(94) | 2.08 (3) |
| Fe(30)–C(9) | 2.05 (3) | Fe(90)–C(59) | 2.05 (3) | Fe(30)–C(35) | 2.07 (4) | Fe(90)–C(95) | 1.99 (4) |
| Fe(30)–C(10) | 2.09 (3) | Fe(90)–C(60) | 2.18 (3) | | | | |
| (b) Intramolecular C–C Distances and C–C–C Angles | | | | | | | |
| C(1)–C(2) | 1.40 (3) | C(51)–C(52) | 1.46 (4) | C(10)–C(11) | 1.48 (4) | C(60)–C(61) | 1.42 (5) |
| C(1)–C(6) | 1.38 (4) | C(51)–C(56) | 1.44 (4) | C(11)–C(12) | 1.43 (4) | C(61)–C(62) | 1.38 (5) |
| C(1)–C(7) | 1.44 (4) | C(51)–C(57) | 1.44 (4) | C(12)–C(13) | 1.43 (4) | C(62)–C(63) | 1.42 (5) |
| C(2)–C(3) | 1.46 (4) | C(52)–C(53) | 1.45 (4) | C(14)–C(15) | 1.45 (5) | C(64)–C(65) | 1.38 (4) |
| C(2)–C(20) | 1.37 (4) | C(52)–C(70) | 1.42 (4) | C(15)–C(16) | 1.36 (5) | C(65)–C(66) | 1.37 (4) |
| C(3)–C(4) | 1.42 (4) | C(53)–C(54) | 1.48 (4) | C(16)–C(17) | 1.49 (4) | C(66)–C(67) | 1.41 (4) |
| C(3)–C(17) | 1.43 (4) | C(53)–C(67) | 1.39 (4) | C(17)–C(18) | 1.41 (4) | C(67)–C(68) | 1.41 (4) |
| C(4)–C(5) | 1.46 (4) | C(54)–C(55) | 1.49 (4) | C(18)–C(19) | 1.41 (4) | C(68)–C(69) | 1.41 (4) |
| C(4)–C(14) | 1.36 (4) | C(54)–C(64) | 1.42 (4) | C(19)–C(20) | 1.47 (4) | C(69)–C(70) | 1.43 (5) |
| C(5)–C(6) | 1.45 (4) | C(55)–C(56) | 1.46 (4) | C(31)–C(32) | 1.47 (5) | C(91)–C(92) | 1.37 (5) |
| C(5)–C(13) | 1.38 (4) | C(55)–C(63) | 1.35 (4) | C(31)–C(35) | 1.48 (5) | C(91)–C(94) | 1.37 (5) |
| C(6)–C(10) | 1.49 (4) | C(56)–C(60) | 1.42 (4) | C(32)–C(33) | 1.38 (5) | C(92)–C(93) | 1.44 (5) |
| C(7)–C(8) | 1.42 (4) | C(57)–C(58) | 1.41 (4) | C(33)–C(34) | 1.42 (5) | C(93)–C(95) | 1.43 (5) |
| C(8)–C(9) | 1.34 (4) | C(58)–C(59) | 1.43 (5) | C(34)–C(35) | 1.44 (5) | C(94)–C(95) | 1.51 (5) |
| C(9)–C(10 | 1.43 (4) | C(59)–C(60) | 1.41 (4) | | | | |
| C(2)–C(1)–C(6) | 121 (2) | C(52)–C(51)–C(56) | 122 (2) | C(6)–C(10)–C(9) | 118 (2) | C(56)–C(60)–C(59) | 119 (3) |
| C(2)–C(1)–C(7) | 120 (2) | C(52)–C(51)–C(57) | 118 (2) | C(6)–C(10)–C(11) | 120 (2) | C(56)–C(60)–C(61) | 120 (3) |
| C(6)–C(1)–C(7) | 118 (2) | C(56)–C(51)–C(57) | 120 (2) | C(9)–C(10)–C(11) | 122 (3) | C(59)–C(60)–C(61) | 122 (3) |
| C(1)–C(2)–C(3) | 119 (2) | C(51)–C(52)–C(53) | 120 (2) | C(10)–C(11)–C(12) | 120 (3) | C(60)–C(61)–C(62) | 120 (3) |
| C(1)–C(2)–C(20) | 120 (3) | C(51)–C(52)–C(70) | 122 (2) | C(11)–C(12)–C(13 | 118 (3) | C(61)–C(62)–C(63) | 120 (3) |
| C(3)–C(2)–C(20) | 120 (3) | C(53)–C(52)–C(70) | 118 (2) | C(5)–C(13)–C(12) | 125 (3) | C(55)–C(63)–C(62) | 121 (3) |
| C(2)–C(3)–C(4) | 119 (3) | C(52)–C(53)–C(54) | 119 (2) | C(4)–C(14)–C(15) | 116 (3) | C(54)–C(64)–C(65) | 123 (2) |
| C(2)–C(3)–C(17) | 121 (3) | C(52)–C(53)–C(67) | 124 (2) | C(14)–C(15)–C(16) | 123 (3) | C(64)–C(65)–C(66) | 119 (2) |
| C(4)–C(3)–C(17) | 119 (3) | C(54)–C(53)–C(67) | 116 (2) | C(15)–C(16)–C(17) | 120 (3) | C(65)–C(66)–C(67) | 121 (2) |
| C(3)–C(4)–C(5) | 121 (3) | C(53)–C(54)–C(55) | 121 (2) | C(3)–C(17)–C(16) | 116 (3) | C(53)–C(67)–C(66) | 123 (2) |
| C(3)–C(4)–C(14) | 125 (3) | C(53)–C(54)–C(64) | 117 (2) | C(3)–C(17)–C(18) | 118 (3) | C(53)–C(67)–C(68) | 116 (3) |
| C(5)–C(4)–C(14) | 114 (3) | C(55)–C(54)–C(64) | 121 (2) | C(16)–C(17)–C(18) | 126 (3) | C(66)–C(67)–C(68) | 122 (2) |
| C(4)–C(5)–C(6) | 116 (2) | C(54)–C(55)–C(56) | 118 (2) | C(17)–C(18)–C(19) | 121 (3) | C(67)–C(68)–C(69) | 123 (3) |
| C(4)–C(5)–C(13) | 124 (3) | C(54)–C(55)–C(63) | 122 (2) | C(18)–C(19)–C(20) | 121 (3) | C(68)–C(69)–C(70) | 120 (3) |
| C(6)–C(5)–C(13) | 120 (2) | C(56)–C(55)–C(63) | 120 (2) | C(2)–C(20)–C(19) | 119 (3) | C(52)–C(70)–C(69) | 118 (3) |
| C(1)–C(6)–C(5) | 123 (2) | C(51)–C(56)–C(55) | 121 (2) | C(32)–C(31)–C(35) | 106 (3) | C(92)–C(91)–C(94) | 112 (3) |
| C(1)–C(6)—C(10) | 120 (2) | C(51)–C(56)–C(60) | 121 (2) | C(31)–C(35)–C(34) | 110 (3) | C(93)–C(95)–C(94) | 106 (3) |
| C(5)–C(6)–C(10) | 117 (2) | C(55)–C(56)–C(60) | 118 (2) | C(31)–C(32)–C(33) | 106 (3) | C(91)–C(92)–C(93) | 108 (3) |
| C(1)–C(7)–C(8) | 122 (3) | C(51)–C(57)–C(58) | 118 (3) | C(32)—C(33)–C(34) | 114 (3) | C(92)–C(93)–C(95) | 107 (3) |
| C(7)–C(8)–C(9) | 121 (3) | C(57)–C(58)–C(59) | 122 (3) | C(33)–C(34)–C(35) | 104 (3) | C(91)–C(94)–C(95) | 106 (3) |
| C(8)–C(9)—C(10) | 121 (3) | C(58)–C(59)–C(60) | 120 (3) | | | | |

reaction was not found at 140 °C and was not investigated at higher temperature. Bimetallic complexes are accessible in the cases of biphenyl, phenanthrene, and triphenylene as well and will be reported later in detail. The yields are much lower than with $FeCp^+$ for the fused polyaromatics. The reaction with coronene (which gives low yields for $FeCp^+$) is not yet clear in the case of FeCp* and its study is in progress. The reaction with perylene gives a mixture of two hydrogenated products, but not the desired non-hydrogenated complex.

Finally, polyaromatics are clearly more difficult to complex by "$CpFe^+$" or "$C_5Me_5Fe^+$" than monoaromatics. Contrary to the reaction with monoaromatics, the complexation of fused polyaromatics is not improved by addition of water to the reaction medium.

**II. X-ray Crystal Structure of the Perylene Complex 9.** [FeCp($\eta^6$-perylene)]$^+PF_6^-$ is so light sensitive that workup needs be performed rapidly in the absence of ambient light. Recrystallization is effected by using acetone and small amounts of ether.

Two distinct conformations are present in the unit cell, as can be seen in Figure 1, which shows the two independent molecules projected on their perylene plane. They correspond to two possible conformations of a mixed $C_5$–$C_6$ sandwich. In the first one, one $C_5$ carbon is located above a $C_6$ carbon; in the second one, a $C_5$ C–C bond is located above a $C_6$ C–C bond. In both arrangements, the complexed $C_6$ ring is located on the outskirt of the perylene nucleus, the central ring having less electron density. Selected bond distances and results of least-square plane calculations are reported in Tables I and II, respectively. The metal–Cp distance is 1.62–1.63 Å; it is slightly shorter than that of other 18-electron $d^6$ $Fe^{II}$ sandwiches such as FeCp($\eta^5$-$C_6Me_5CH_2$)[29] and $Fe^{II}Cp(\eta^6$-$C_6Et_6)PF_6$[30] (1.68 Å for both). The metal–arene distance is 1.56–1.57 Å, which is 0.02 Å longer than in the two complexes above. The rings are planar and parallel, and there is no shift of the metal to one side that would indicate partial decoordination, $\eta^6 \rightarrow \eta^4$.

**III. Electrochemistry.** For all of the monocations studied, except **8** and **10**, the electrochemistry is similar. In DMF, at −30 °C, two reductions occur well negative of the SCE and are separated by 0.5–0.8 V (see Table III). The first reduction (+/0) of complexes **1**–**7** and **11**–**18** is shown to be diffusion controlled since cyclic voltammetry measurements between 30 and 500 mV/s show that $ip/v^{1/2}$ is constant.[31] At these scan rates, the $E_p$ value is typically 50–60 mV, indicating a nearly reversible electron transfer.

(29) Hamon, J. R.; Astruc, D.; Román, E.; Batail, P.; Mayerle, J. J. *J. Am. Chem. Soc.* **1981**, *103*, 2431.
(30) Hamon, J. R.; Saillard, J. Y.; Le Beuze, A.; McGlinchey, M.; Astruc, D. *J. Am. Chem. Soc.* **1982**, *104*, 7549.
(31) Bard, A. J.; Faulkner, L. R. *Electrochemical Methods*; Wiley: New York, 1980.

**Table II. Weighted Least-Square Planes for [FeCp(perylene)]$^+PF_6^-$**

| plane 1[a] | | plane 2[b] | | plane 3[c] | | plane 4[d] | |
|---|---|---|---|---|---|---|---|
| atom | dist, Å | atom | dist, Å | atom | dist, Å | atom | dist, Å |
| | | | Atoms in the Plane | | | | |
| C(1) | −0.0119 | C(31) | 0.0082 | C(51) | 0.0314 | C(91) | 0.0260 |
| C(6) | −0.0039 | C(32) | −0.0080 | C(56) | −0.0001 | C(92) | −0.0400 |
| C(7) | −0.0001 | C(33) | 0.0048 | C(57) | −0.0253 | C(93) | 0.0380 |
| C(8) | 0.0304 | C(34) | 0.0008 | C(58) | −0.0126 | C(94) | −0.0012 |
| C(9) | −0.0467 | C(35) | −0.0057 | C(59) | 0.0446 | C(95) | −0.0229 |
| C(10) | 0.0323 | | | C(60) | −0.0380 | | |
| | | | Other Atoms | | | | |
| Fe(30) | −1.5722 | Fe(30) | 1.6274 | Fe(90) | 1.5616 | Fe(90) | −1.6228 |

[a-d] The equations of the planes are as follows: [a] $(0.4929)X + (-0.1741)Y + (0.8525)Z = 10.7287$. [b] $(0.4975)X + (-0.1739)Y + (0.8498)Z = 7.5368$. [c] $(-0.2091)X + (0.9675)Y + (0.1419)Z = 3.7795$. [d] $(-0.2136)X + (0.9593)Y + (0.1848)Z = 7.3432$. $X$, $Y$, and $Z$ are orthogonalized coordinates.

**Table III. Electrochemical Data[a]**

| | | first reductn potential | | | second reductn potential |
|---|---|---|---|---|---|
| | Cp | $E°_1$ | $i_a/i_c$ | $d$ on Ar, % | $E°_2$ |
| 1 | benzene | −1.36 | 0.8 | 10–15 | −2.10 |
| 2 | biphenyl | −1.27 | 0.8 | 10–30 | −1.97 |
| 5 | naphthalene | −1.00 | 0.9 | 15–35 | −1.54 |
| 6 | phenanthrene | −1.07 | 0.83 | 40–60 | −1.67 |
| 7 | triphenylene | −1.14 | 0.77 | 10–30 | −1.68 |
| 8 | pyrene | −1.10 ($E_p$) | 0 | 55–75 | |
| 9 | perylene | −0.8 | 0.73 | 70–90 | −1.24 |
| 10 | coronene | −1.07 | 0 | 80–100 | |
| | | first reductn potential | | | second reductn potential |
| | Cp* | $E°_1$ | $i_a/i_c$ | $d$ on Ar, % | $E°_2$ |
| 11 | benzene | −1.64 | 0.9 | 15–30 | −2.40 |
| 12 | biphenyl | −1.57 | 0.96 | 15–30 | −2.33 |
| 15 | naphthalene | −1.28 | 1 | 15–30 | −1.84 |
| 16 | phenanthrene | −1.36 | 0.75 | 15–30 | −2.04 |
| 17 | triphenylene | −1.43 | 0.95 | 15–30 | −2.20 |
| 18 | pyrene | −1.32 | 0.85 | 15–30 | −1.84 |

[a] $E°$ values are the thermodynamic redox potentials in V vs SCE determined by cyclic voltammetry (DMF, 0.1 M $Bu_4N^+BF_4^-$, Hg cathode, −30 °C). The $i_a/i_c$ values show the reversibility of the first reduction at a scan rate of 0.3 V $s^{-1}$. The $d$ value is the ratio found in Vlček's equation (see text) and gives the arene character in the SOMO (compare with the values found from extended Hückel and X$\alpha$ calculations, Table IV). The $d$ values are calculated in an iterative way using two arenes which have close $d$ values. For a given arene, the reported $d$ value is the average of values found using several arenes. These $d$ values are close to the spin density values on the polyaromatic ligands. The $E°$ values of various polyaromatics used to calculate $d$ are found in ref 35. Values for the second reduction ($E°_2$) are approximate since the degree of electrochemical reversibility is weaker for polyaromatic complexes; $E°_2$ values are not given when $i_a/i_c = 0$ even at high scan rates.

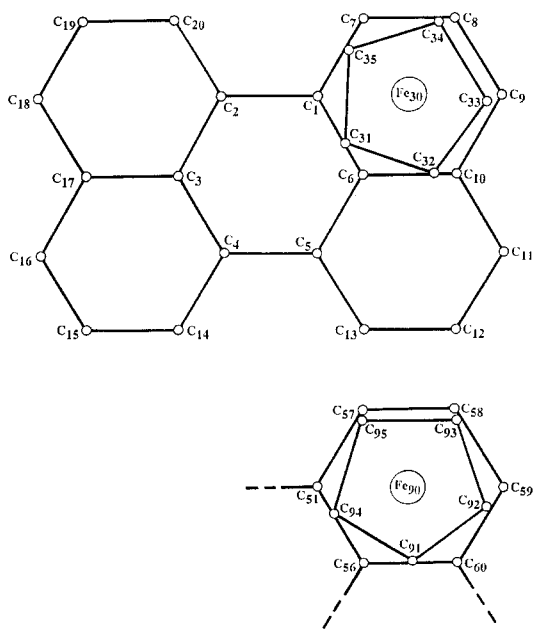


**Figure 1.** Projection of the sandwiches normal to the perylene planes. The numbering of the perylene carbons in molecule 2 are obtained by adding 50 to the corresponding atoms in the molecule.

(At −30 °C, a reversible electron transfer is expected to have a $\Delta E_p$ of 49 mV. Ferrocene, under these conditions, had a $\Delta E_p$ of 50 mV.)[21] At $v$ = 100 mV/s., $i_a/i_c$ is always 1, indicating a stable reduced species on this time scale. Complexes **8** and **10** were the only ones with exceptional results. The first reduction is chemically irreversible, and the reported potential is $E_p$ at $v$ = 100 mV/s.

The second reduction (0/−) is similarly shown to be diffusion controlled for complexes **1**–**7** and **11**–**18**. However, the $\Delta E_p$ values are considerably larger (100–300 mV) than for the first reduction, indicating a slower heterogeneous electron transfer. Consistent with this, the currents of the second wave are 0.7–0.9 times smaller than for the first wave. When solvent reduction was not interfering, $i_a/i_c \approx 1$ at $v$ = 100 mV/s. Thus these data are consistent with the reported electrochemistry of other [FeCp(arene)]$^+$ complexes.[16-21]

The ligand character d in the LUMO of the complexes can be calculated by using Vlček's[32] theory if thermodynamic reduction potentials in both series of free ligands and complexes are available. This requirement adapts well to polyaromatics that are reversibly reducible as are their

(32) (a) Vlček, A. A. *Z. Anorg. Allg. Chem.* **1960**, *304*, 109. (b) Vlček, A. A. *Collect. Czech. Chem. Commun.* **1965**, *30*, 952.

complexes. Vlček's relation (eq 3) applies to two distinct ligands, $L_1$ and $L_2$, within the same family of complexes

$$d = \frac{E_{1/2}(ML_1) - E_{1/2}(ML_2)}{E_{1/2}(L_1) - E_{1/2}(L_2)} \quad (3)$$

where M is a metal atom or a metallic fragment.

To establish this equation, Vlček[32] assumed that the complex molecular orbital (MO) involved in the reduction process could be written as a linear combination of two fragment orbitals

$$\psi_{ML} = C_M\phi_M + C_L\phi_L$$

its energy being $\epsilon_{ML} = \langle\psi|\hat{h}|\psi\rangle = C_M{}^2H_{MM} + C_L{}^2H_{LL} + 2C_MC_LH_{ML}$, where $H_{IJ} = \langle\phi_I|\hat{h}|\phi_J\rangle$ ($\hat{h}$ = one-electron effective Hamiltonian of the system).

Considering two complexes differing only by the nature of their electronically closely related L ligands, Vlček assumed that $C_M$, $C_L$, and $H_{ML}$ are constant when going from $ML_1$ to $ML_2$. It then follows

$$\epsilon_{ML_1} - \epsilon_{ML_2} \simeq C_L{}^2[H_{LL}{}^1 - H_{LL}{}^2] \simeq C_L{}^2(\epsilon_{L_1} - \epsilon_{L_2})$$

where $\epsilon_L$ is the one-electron energy of orbital $\phi_L$ in the free ligand L. Neglecting the $C_H$, $C_L$, and $H_{ML}$ terms, the quantity $C_L{}^2 = (\epsilon_{ML_1} - \epsilon_{ML_2})/(\epsilon_{L_1} - \epsilon_{L_2})$ represents the L localization of the $\psi_{ML}$ molecular orbital.

Since for two closely related substances there is a relation between the energy difference of their LUMO's and the difference of their reduction potentials (if determined in similar conditions), i.e. $\Delta\epsilon \propto -\Delta E_{1/2}$, eq 3 is then demonstrated.

Because of the various approximations, eq 3 must be considered as only giving an estimation of the LUMO localization on L.[32] In particular, it should be emphasized that the validity of this relation is expected to fall when (i) the $L_1$ and $L_2$ ligands are electronically too different. In order to minimize the errors, it is then necessary to proceed cautiously stepwise when exploring a series of complexes and (ii) it is not the same $\phi_L$ ligand orbital that is involved in the reduction of L and ML. For example, when L = arene, the orbital involved when reducing the free ligand is an antibonding $\pi^*$ MO. It is then necessary that the accepting ML LUMO has a $\pi^*$ L contribution. Actually, it appears that, in his original paper,[32] Vlček applied his equation in the wrong case. Indeed, he assumed that the accepting level implied when reducing 17-electron compounds of the type $(arene)_2Cr^+$ was a bonding combination of Cr $d_\pi$ and $\pi^*$ arene fragment MO's. Since then, it has been well established[33] that the right level is of Cr $d_{z^2}$ nature, with an antibonding contribution of the highest $\pi$-bonding arenic MO. Surprisingly, Vlček's result ($d$ = 16% on both ligands) is in good agreement with the ones obtained by recent sophisticated theoretical calculations on $(C_6H_6)_2Cr$ ($d$ = 13–23%).[33,34] This apparent contradiction can be rationalized by considering that, when one goes from one arene to another one, the $\pi$-MO levels are all pushed up (or down) by an energy shift of the same order of magnitude. If such a condition is fulfilled, the $\epsilon_{L_1} - \epsilon_{L_2}$ and then the $E_{1/2}(L_1) - E_{1/2}(L_2)$ denominators are independent of the nature of the ligand MO involved in the reduction. Such a situation was implicitely suggested by Vlček,[32] who also replaced the $\Delta E_{1/2}(L)$ denominator of eq 3 by a term depending on the electronegativity difference between two ligands. His result, $d$ = 12%, is close to the one he found by using the unmodified eq 3.

**Chart II**

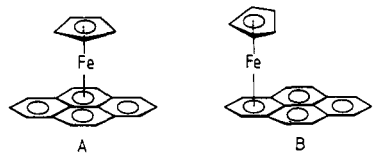


Later, in the series of 18-electron $[FeCp(arene)]^+$ complexes, Gubin et al. calculated the value of 20% for spin density $d$ on the arene ligand in the 19-electron reduced complexes.[9] Again, in this case, this is not the same arenic MO that is involved during the reductions of the free arene and of the complex (see Figure 2 and vide infra). It then appears that eq 3 remains valid in such a case, although probably leading to a cruder estimate. Gubin et al. reported a single $d$ value for the whole series of complexes whereas we indicate in the present study that considerable variations in $d$ values are found. In addition, it was found after Gubin's work that polyaromatic ligands used in his study were, in fact, hydrogenated.[11-13]

Following Gubin et al., we have determined the LUMO localization of our $Fe^{II}$ complexes, using eq 3. Our results are given in Table III. We calculated the denominator of eq 3 by using the literature data.[35,36] The spin density increases from 10–30% for biphenyl (and monoaromatic) to 80–100% for coronene, i.e. progressively as the number of fused rings increases in the polyaromatic coordinated to $(FeCp)^+$. This is not the case, however, for the permethylated complexes we could study.

For this latter series, only a common $d$ value of 15–20% could be estimated for the whole series. Contrary to the Cp series, no complex could be made yet with more than four rings, which would give a monoreduced state with high-spin density on the ligand. Under such conditions, one cannot compare the $d$ values for the Cp and the Cp* complexes of phenanthrene and pyrene.

**IV. Theoretical Study. Extended Hückel (EH) Calculations.** EH calculations have been performed on the CpFe complexes of benzene, naphthalene, phenanthrene, triphenylene, pyrene, perylene, and coronene. The geometries of all of these compounds have been modeled on the experimental structure of $CpFe(C_6Me_6)$[28a] (see Appendix), with the two planar ligands considered parallel and one of the Cp carbon atom eclipsing the middle of a C–C arenic bond (conformation $C_5$). In the case of polyaromatics having more than two fused rings, an external cycle has been chosen to be complexed by the metal atom, as usually observed in the complexes of polyaromatic ligands. In the special case of CpFe(pyrene), both conformations A and B (Chart II) have been considered, since our EH calculations give A slightly more stable than B (by only 0.04 eV), while for the 18-electron $Fe^{II}$ cation B is, as expected, more stable by 0.31 eV. The symmetry group

(33) (a) Weber, J.; Geoffroy, M.; Goursot, A.; Penigault, A. *J. Am. Chem. Soc.* **1978**, *100*, 3395. (b) Weber, J.; Kundig, E. P.; Goursot, A.; Penigault, A. *Can. J. Chem.* **1985**, *63*, 1734. (c) Osborne, J. H.; Trogler, W. C.; Morand, P. C.; Francis, C. G. *Organometallics* **1987**, *6*, 94.

(34) Simple EH calculations on $(C_6H_6)_2Cr$ lead to a 10% benzene participation in the $a_{1g}$ ($d_{z^2}$) HOMO. Rabaâ, H.; Saillard, J. Y., unpublished results.

(35) (a) Dewar, M. J. S.; Hashmall, J. A.; Trinajstic, N. *J. Am. Chem. Soc.* **1970**, *92*, 5555. (b) Notoya, R.; Matsadan, A. *J. Res. Inst. Catal., Hokkaido Univ.* **1981**, *29*, 67. (c) Bank, S.; Juckett, D. A. *J. Am. Chem. Soc.* **1976**, *98*, 7742. (d) Hoijink, G. J. *Recl. Trav. Chim. Pays-Bas* **1955**, *74*, 1525. (e) Hoijink, G. J.; Van Schooten, J. *Recl. Trav. Chim. Pays-Bas* **1954**, *73*, 355. (f) Gough, T. A.; Peover, M. E. In *Polarography*, Proceedings of the 3rd International Conference, Southampton; Hills, G. J., Ed.; MacMillan; New York, 1964; Vol. 2, p 1017. (g) Brieglet, G. *Angew. Chem., Int. Ed. Engl.* **1964**, *3*, 617. (h) Kojima, H.; Bard, A. J. *J. Am. Chem. Soc.* **1975**, *97*, 6317.

(36) (a) It is satisfactory to note that the differences between the reduction potentials of two given polyaromatics are rather constant among the reports.[35] (b) Desbois, M.-H.; Astruc, D.; Guillin, J.; Varret, F.; Trautwein, A. X.; Villeneuve, G. *J. Am. Chem. Soc.* **1989**, *111*, 000.

(37) Green, J. F.; Kelly, M. R.; Payne, M. P.; Seddon, E. A.; Astruc, D.; Hamon, J. R.; Michaud, P. *Organometallics* **1983**, *2*, 211.

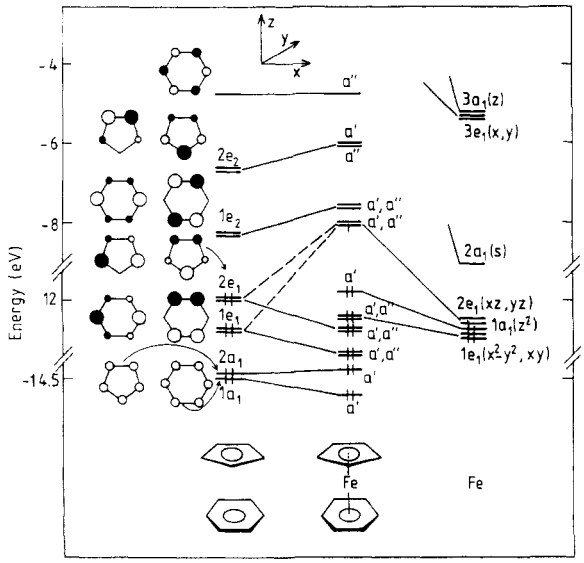


**Figure 2.** MO interaction diagram of CpFe(benzene), as obtained by EH calculations.

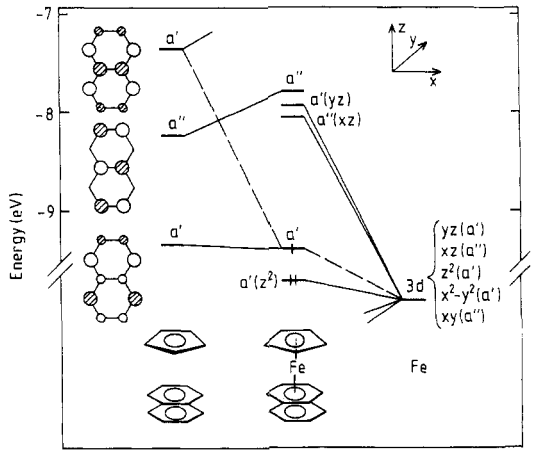


**Figure 3.** MO interaction diagram of CpFe(naphthalene), as obtained by EH calculations. Only the levels lying in the HOMO/LUMO region are shown.

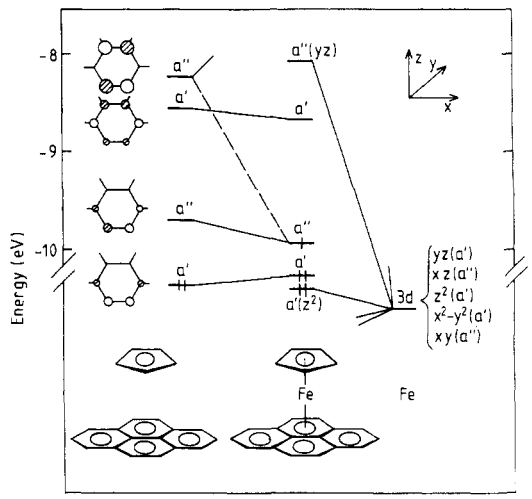


**Figure 4.** MO interaction diagram of CpFe(pyrene) (conformation A), as obtained by EH calculations. Only the levels lying in the HOMO/LUMO region are shown.

of all the studied complexes is $C_s$, except for the complexes of phenanthrene and perylene where it is $C_1$.

We start our analysis with the well-known[24] electronic structure of CpFe(benzene), taken as a reference for the other complexes. It can be analyzed on the basis of the interaction between the fragment molecular orbitals (FMO's) of the Cp and benzene ligands on one side and of the iron atom on the other side, as shown on Figure 2. In the cylindrical $C_{\infty v}$ strong pseudosymmetry of the complex, the major bonding interactions are of the $e_1(\pi)$ and $e_2(\delta)$ types: the occupied $e_1$ $\pi$-bonding orbitals of the two ligands are stabilized by the $x, y$ and $xz, yz$ iron AO's while the $e_2$ $\pi^*$-antibonding ligands FMO's stabilize the $x^2 - y^2$ and $xy$ iron AO's. As a result of their interaction with the ligand $e_1$ levels, the iron $xz$ and $yz$ orbitals are destabilized and become the lowest antibonding MO's of the complex, lying below the $e_2$ level derived from the benzene FMO's.[38] In the neutral $Fe^I$ complex, the single electron occupies this doubly degenerate level of $xz$, $yz$ dominant character (53%). Because the Cp orbitals lie at higher energy than the ones of benzene, this singly occupied level has a larger localization on Cp (30%) than on benzene (17%). This MO level ordering is fully consistent with all the experimental data reported on this type of complex[24,37] and with recent X$\alpha$ calculations[39] (vide infra).

Compared with benzene, a polyaromatic molecule has a larger set of $\pi$ MO's, delocalized over several rings, and with a smaller $\pi/\pi^*$ energy gap. This difference from benzene is expected to increase with the size of the polyaromatic. Despite these differences and the lowering of pseudosymmetry when going from CpFe(benzene) to CpFe(polyaromatic) complexes, the major interactions are rather similar. In particular the $x^2 - y^2$ and $xy$ Fe atomic orbitals are stabilized by the $\pi^*$ ligand (mainly arenic) MO's and the $xz$ and $yz$ iron AO's are destabilized by the $\pi$ ligand (mainly Cp) orbitals. However, a major change is found by our EH calculations in the nature of the singly occupied molecular orbital (SOMO) of the complexes, which is largely of arenic character when arene is polyaromatic (see Figures 3 and 4 and Table IV). Indeed, the low-lying, weakly antibonding LUMO of any of the polyaromatics investigated because of its delocalization and of its nodal properties, overlaps weakly with the iron AO's. Moreover, a second-order mixing occurs with a higher $\pi^*$ arenic MO (see, for example, Figures 3 and 4) relocalizing it on the uncomplexed rings. As a consequence, the lowest antibonding level, which is the SOMO of the neutral complexes, is no longer generated by the $d_\pi$ iron AO's as in the benzene complex but by the polyaromatic LUMO (see Table IV).

For all the complexes investigated, the lowest vacant level having a significant metal character lies far above the SOMO; its lowest position (~1 eV above the SOMO) is observed in the case of the complexes of naphthalene, phenanthrene, and triphenylene. For these three latter compounds, the calculated amounts of arene character (Table IV) disagree with the corresponding experimental values (Table III). However, the trend in the calculated SOMO energy is in good accord with the trend in the reduction potentials observed for the three compounds. At this point of the discussion, it should be noted that the EH results are not parameter dependent: The SOMO remains preferentially localized on the arenic ligand when the iron $H_{ii}$'s are varied (±2 eV) or when reasonable changes in bond distance are applied. In particular a shift

(38) The $d_\pi < \pi^*$(benzene) level ordering accommodates the classical sandwich structure in CpFe(benzene) and related complexes, with dynamic (not static) Jahn–Teller activity. Conversely the reverse ordering in $(C_6H_6)Cr$ is responsible of the benzene static distortion ($\eta^6,\eta^4$ coordination) observed in its reduced monoanion; see: Elschenbroich, C.; Bilger, E.; Koch, J. *J. Am. Chem. Soc.* **1984**, *106*, 4297 and references therein.

(39) (a) Le Beuze, A.; Lissillour, R.; Roch, M.; Weber, J., to be submitted for publication. (b) Le Beuze, A.; Lissillour, R.; Weber, J., to be submitted for publication.

**Table IV. Localization of the Singly Occupied MO of CpFe(aromatic) Complexes as Calculated by the Extended Hückel and SCF-MS-Xα Methods**

| | extended Hückel calculations | | | | | | | SCF-MS-Xα calculations CpFe[I](arene) SOMO[a] | | | | | |
|---|---|---|---|---|---|---|---|---|---|---|---|---|---|
| | | CpFe[I](arene) SOMO | | | | | | | | | | | |
| | free arene LUMO energy, eV | energy, eV | symmetry | % arenic LUMO participation | % arene (total) | % Fe | % Cp | % arene | % Fe | % Cp | % arene | % Fe | % Cp |
| CpFe(benzene) | −8.35 | −8.07 | $e_1(a',a'')$ | 0 | 17 | 53 | 30 | 8 | 73 | 19 | 9 | 67 | 20 |
| CpFe(naphthalene) | −9.34 | −9.38 | a′ | 68 | 80 | 13 | 7 | 35 | 47 | 18 | 42 | 32 | 18 |
| CpFe(phenanthrene) | −9.31 | −9.29 | a | 79 | 87 | 9 | 4 | | | | | | |
| CpFe(triphenylene) | −9.06 | −9.06 | a′ | 80 | 91 | 6 | 3 | | | | | | |
| CpFe(pyrene)[b] | −9.70 | −9.94 | a″ | 79 | 86 | 9 | 5 | 63 | 25 | 12 | 69 | 17 | 14 |
| CpFe(pyrene)[c] | −9.70 | −9.59 | a″ | 85 | 90 | 7 | 3 | | | | | | |
| CpFe(perylene) | −9.97 | −9.92 | a | 86 | 91 | 6 | 3 | | | | | | |
| FeCp(coronene) | −9.42 | −9.57 | a″ | 76 | 85 | 9 | 5 | | | | | | |

[a] Left side: the inner- and outer-sphere charges have been partitioned on the three arene, Cp, and Fe units. [b] Conformation B. [c] Conformation A.

of the FeCp moiety away from the center of the complexed ring and the use of various experimental geometries of the free polyaromatic ligands were tested.

**SCF-MS-Xα Calculations.** In order to check the validity of our EH results, we then undertook the determination of the electronic structure of the CpFe complexes of naphthalene and pyrene using a more sophisticated method, which has been proven to be particularly useful for the rationalization of the bonding in closed- and open-shell sandwich complexes.[33a,b,40] Moreover, similar calculations by one of us, on the reference complex CpFe(benzene), are available.[39] The choice of the A conformation for CpFe(pyrene) (Chart II) was dictated by our EH results and by the possibility of using the converged results of CpFe(naphthalene) in the starting potential. The three energy diagrams are given in Figure 5, where the molecular levels of the three complexes are correlated with respect to their main character (Fe, Cp, or arene). In order to make the results comparable, the three MO diagrams have been adjusted by placing their essentially nonbonding Fe $3d_\sigma$ ($z^2$) level at the same energy. By using this rescaling procedure, one can avoid the energy shift between the levels of the different complexes which is an artifact of the "muffin-tin" approximation.

In Table IV are summarized the SOMO charge distribution obtained by two ways of partitioning the inner- and outer-sphere charges on the Fe, Cp, and arene units: a partition on the three units proportionally to the already calculated charges and a partition on the Cp and arene ligands exclusively.

The results obtained for CpFe(benzene)[39] (see Figure 5 and Table IV) are qualitatively similar to those obtained by EH calculations with the following level ordering: $\pi$(benzene) < $\pi$(Cp) < Fe($x^2-y^2$, $xy$) < Fe($z^2$) ≪ HOMO Fe($xz$, $yz$) < $\pi^*$(benzene).

The doubly pseudodegenerate level (13a″, 20a′) which contains the single electron is mainly metallic, as also found when applying Vlček's theory to our voltammetric results, and it has a very small benzene participation.[39]

Reasonable agreement is also found between the two types of calculations on the A conformation of CpFe(pyrene). In both cases, the a″ SOMO is found preferentially localized on the arenic ligand with some iron (mainly $xz$) character (Table IV). Also in agreement with EH

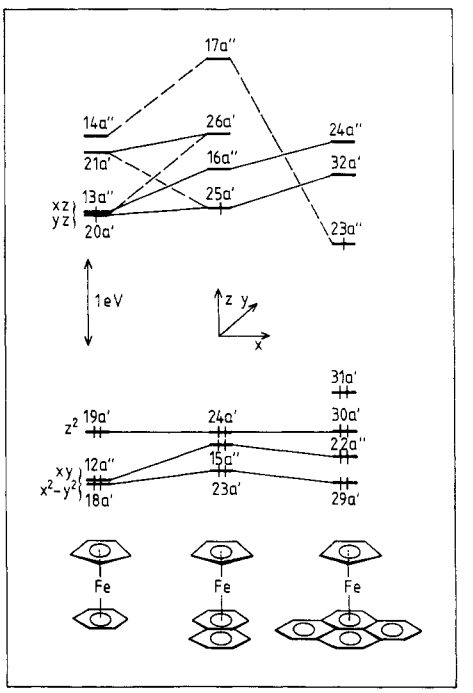


**Figure 5.** Correlation diagram of the crucial MO levels obtained by Xα calculations on benzene, naphthalene, and pyrene complexes.

results, a smaller electron density is found on the ring which is complexed by the iron atom: only 3% of the 46% localization on the pyrene ligand is from the complexed ring.

Considering both EH and Xα data on CpFe(pyrene), it seems probable that Xα calculations on the B conformation of the complex would give an MO picture qualitatively similar to the one obtained for conformation A; i.e. in both conformations the SOMO is mainly localized on the arenic ligand (60–70%). Then, whatever the conformation of CpFe(pyrene), there is a reasonable concordance between the experimental (Table IV) and theoretical results.

Both types of calculations, however, disagree in the case of CpFe(naphthalene). Contrary to what is found by EH calculations, the 25a′ HOMO is strongly delocalized on the iron atom *and* the naphthalene ligand, with a larger iron participation (mainly $yz$). In the naphthalene complex, like in the benzene complex, the formal metal configuration is $d^7$ ($Fe^I$, 19 electrons), but in the former case the SOMO is much more delocalized on the arenic ligand (Table IV). We then checked the conservation of this $d^7$ configuration with respect to a change in the Fe–Cp distance. Indeed, according to our Xα calculations, the 25a′ MO is nonbonding between the Fe atom and the naphthalene and has a small Cp character. When going from CpFe(benzene) to CpFe(naphthalene), there is a loss of Fe–Cp antibonding

(40) (a) Rösch, N.; Klemperer, W. G.; Johnson, K. H. *Chem. Phys. Lett.* **1973**, *23*, 149. (b) Case, D. A.; Karplus, M. *J. Am. Chem. Soc.* **1977**, *99*, 6132. (c) Goursot, A.; Penigault, E.; Weber, J. *Nouv. J. Chim.* **1979**, *3*, 675. (d) Case, D. A.; Huynh, B. H.; Karplus, M. *J. Am. Chem. Soc.* **1979**, *101*, 433. (e) Norman, J. G., Jr.; Renzoni, G. E.; Case, D. A. *J. Am. Chem. Soc.* **1979**, *101*, 5256. (f) Anderson, E. L.; Fehlner, T. P.; Foti, A. E.; Salahub, D. R. *J. Am. Chem. Soc.* **1980**, *102*, 7422. (g) Sunil, K. K.; Rogers, M. T. *Inorg. Chem.* **1981**, *20*, 3233. (h) Weber, J.; Goursot, A.; Penigault, E.; Ammeter, J. H.; Bachman, J. *J. Am. Chem. Soc.* **1982**, *104*, 1491. (i) Perfiled, K. W.; Gervith, A. A.; Solomon, E. F. *J. Am. Chem. Soc.* **1985**, *107*, 4519.

character, in the same way as when going from $CpFe^{I}$(benzene)[28a] to $[CpFe^{II}(benzene)]^{+}$.[30] By analogy with the molecular structures of these two latter complexes, we undertook a second calculation on CpFe(naphthalene) with a shorter Fe–Cp distance: 1.70 Å in place of 1.78 Å in the other calculations. The results are only slightly different from the ones obtained in the first calculation, despite the rather important geometrical change: the SOMO has now 31% arenic character and 41% Fe character (compare with the 35% and 47% values in Table IV). As in the case of the pyrene complex, and in agreement with our EH results, the SOMO localization on the complexed ring is smaller: only 6% of the 28% localization on the arenic ligand.

Obviously, EH calculations give a wrong ordering of the a′ SOMO and the a′ *yz* LUMO in CpFe(naphthalene) probably because this approximate method underestimates the interaction between the naphthalene LUMO and the iron *yz* atomic orbital. Considering the experimental voltammetric results (Table III), one can think that a similar wrong level ordering is likely to exist in the EH results of the phenanthrene and triphenylene complexes.

**V. Generation of Fe(I) and Monoreduced Complexes.**[28c] Given the instability of monoreduced complexes above −30 °C and the possibility to reduce them further, we considered avoiding alkali metals and Na amalgam to effect specifically the one-electron reduction of the cationic complexes. We know that many complexes of the type $[FeCp(arene)]^{+}$ can be reduced to $Fe^{I}$ analogues by using $LiAlH_4$ in THF at low temperature.[15,24,28c] Further H atom transfer also occurs but at higher temperatures. Thus we used this method to generate the monoreduced complexes of polyaromatics at −80 °C, and color change was immediately observed even though reaction mixtures are heterogeneous. No reduction to the bireduced complexes was ever observed. For example, we know that $[Fe_2Cp_2(fulvalene)(arene)_2]^{2+}$ can be monoreduced by $LiAlH_4$ in THF, but the second reduction to the otherwise well-characterized biradical was never noted.[36b] Thus, we are confident of the monoelectronic reduction of $[FeCp(polyaromatic)]^{+}$ in this way, and, accordingly, ESR spectra recorded always correspond to the monoreduced species. Indeed, most reactions were directly effected in ESR tubes slightly above the freezing point of the THF suspension containing a large excess of $LiAlH_4$ (25 mol/mol of Fe complex); monoelectronic reduction is easily observable by a strong color change from the pale yellow suspension of the cation to the intense, deep color of the soluble radical species.

Complexes of polyaromatic ligands with a number of fused rings lower than (or equal to) four have a relatively high metal character (at least 50%), and their ESR spectra are quite similar to those of $CpFe(C_6H_6)$; i.e., they exhibit three *g* values around 2 due to the rhombic distortion of the Jahn–Teller active species. Complexes of polyaromatic ligands with a number of fused rings greater than four have a low-spin density on the metal and a high-spin density on the polyaromatic. These are by far the most unstable complexes, and their ESR spectra show a single line, thus without hyperfine splitting with the H's.

## Conclusion

This study has improved our understanding of the complexation of polyaromatics by different iron moieties, which renders a broad class of polyaromatic iron complexes amenable to study. The electrochemical and $LiAlH_4$ reduction studies show a varying localization of the spin density as a function of the polyaromatic and ancillary ligand structure. Meanwhile it illustrates the concept of "electron reservoir" which proposed that the localization of the extra electron inside a three-dimensional molecular structure brings about stability of the reduced state.[28] This understanding is essential to the device of stable binuclear electron reservoir systems with polyaromatic bridging ligands that are presently under study in our laboratories.

Taking all the theoretical and experimental results as a whole, it seems reasonable to conclude that CpFe complexes of polyaromatic ligands with a number of fused rings larger than four have a small spin density on the metal and a large spin density on the polyaromatic. Conversely, complexes of polyaromatics having less than four fused rings have a large spin density on the iron. Indeed, the LUMO's of these latter polyaromatics because of their higher energy and larger localization generate, after interaction with the iron 3d orbitals, an unoccupied MO in the complex. Complexes with four fused rings constitute the borderline case. Triphenylene, from its Clar structures,[3a,4b] is expected to adopt a behavior closer to the one of benzene while the more compact pyrene is closely related to, for example, perylene.

## Experimental Section

**General Data.** All manipulations of air-sensitive materials were conducted in a VAC drybox or under argon in Schlenk apparatus connected to a double manifold providing vacuum and dry argon. Reagent grade tetrahydrofuran, pentane, and toluene were predried on Na foil and distilled from sodium benzophenone ketyl under argon. All other chemicals were used as received. $^1H$ NMR spectra were obtained with a Bruker AC 200 spectrometer, and the $^{13}C$ NMR spectra were recorded with a Bruker AC 200 (50.3 MHz) or a Bruker AC 250 (67.9 MHz). NMR spectra were referenced to $Me_4Si$ ($^1H$) or to the appropriate deuteriated solvent ($^{13}C$). Cyclic voltammetry studies were done on a Princeton Applied Research 273. ESR spectra were recorded by using a Bruker ER 20 ttX band spectrometer. Elemental analyses were performed by the CNRS Center of Microanalyses at Lyon-Villeurbanne.

**1. $[FeCp(phenanthrene)]^{+}PF_6^{-}$ (6).** Ferrocene (18.6 g, 100 mmol), Al powder (0.54 g, 20 mmol), $AlCl_3$ (13.4 g, 100 mmol), and phenanthrene (1.8 g, 10 mmol) were stirred under argon in a bottom flask at 80 °C for 15 h. Then the melt layer was hydrolyzed with ice water; $NH_4OH$ was added to the aqueous layer to remove $Al^{3+}$, and aqueous $HPF_6$ (10 mmol) was added to the filtrate to precipitate a yellow powder. Recrystallization from acetone/ether provided 3.7 g (70% yield) of a yellow microcrystalline powder of **6** found pure by $^1H$ NMR. Mössbauer data (mm/s vs Fe, 298 K): IS, 0.45; QS, 1.74. ESR data (77 K, frozen THF solution); $g_x = 2.0683$, $g_y = 1.9988$, $g_z = 1.8807$.

**2. $[FeCp(pyrene)]^{+}PF_6^{-}$ (8).** Ferrocene (18.6 g, 100 mmol), Al powder (0.54 g, 20 mmol), $AlCl_3$ (13.4 g, 100 mmol), and pyrene (2.1 g, 10 mmol) were stirred under argon in a round-bottom flask at 120 °C for 15 h. Workup proceeded as above, yielding 3.61 g (74% yield) of a yellow microcrystalline powder of **8** found pure by $^1H$ NMR. Mössbauer data (mm/s vs Fe, 298 K): IS, 0.48; QS, 1.78.

**3. $[FeCp(triphenylene)]^{+}PF_6^{-}$ (7).** Ferrocene (4 g, 21 mmol), Al powder (0.1 g, 3 mmol), $AlCl_3$ (2.3 g, 17 mmol), and triphenylene (0.5 g, 2.2 mmol) were stirred under argon in a round-bottom flask at 120 °C for 15 h. Workup proceeded as in section 1, yielding 0.8 g (74% yield) of a yellow microcrystalline powder of **7**. $^1H$ NMR ($CD_3CN$, $Me_4Si$): δ 8.7 and 8.56 (m, 4 H, uncomplexed aromatic), 7.88 (m, 4 H, uncomplexed aromatic), 7.04 (m, 4 H, complexed aromatic), 4.46 (s, 5 H, $C_5H_5$) ppm. $^{13}C$ NMR ($C_3D_6O$): δ 132.01, 130, 126, 125.45 (uncomplexed CH), 132.34, 128.8 (uncomplexed C), 88.43, 82.279 (complexed CH), 94.59 (complexed C), 78.64 ($C_5H_5$) ppm. Anal. Calcd for $C_{23}H_{17}FePF_6$: C, 55.87; H, 3.44. Found: C, 55.74; H, 3.43. Mössbauer data (mm/s vs Fe, 298 K): IS, 0.43; QS, 1.58. ESR data (77 K, frozen THF solution): $g_x = 1.9976$, $g_y = 2.0652$, $g_z = 1.8600$.

**4. $[FeCp(coronene)]^{+}PF_6^{-}$ (10).**[28] Ferrocene (2.4 g, 13 mmol), Al powder (0.07 g, 2.5 mmol), $AlCl_3$ (1.8 g, 13 mmol), and coronene (0.4 g, 1.3 mmol) were stirred under argon in a round-bottom flask

at 120 °C for 15 h. Workup proceeded as above, yielding 0.06 g (8% yield) of a red microcrystalline powder of **10** found pure by $^1H$ NMR. This cation is very light sensitive, and all operations had to be carried out in the dark. ESR data (77 K, frozen THF solution): $g = 2.0028$.

**5. [FeCp(perylene)]$^+PF_6^-$ (9).** Ferrocene (3.6 g, 20 mmol), perylene (0.5 g, 2 mmol), $AlCl_3$ (0.8 g, 6 mmol), Al powder (0.05 g, 2 mmol), and $H_2O$ (0.03 g, 2 mmol) were mixed under argon and heated at 180 °C for 16 h in 50 mL of Decalin. After hydrolysis at 0 °C, $NH_4OH$ was added to the aqueous layer to remove $Al^{3+}$, and then aqueous $HPF_6$ (2 mmol) was added to the filtrate to precipitate a red powder of **9**. Reprecipitation by addition of excess ether to a $C_3H_6O$ solution provided 0.1 g (10% yield) of powdered salt of **9** found pure by $^1H$ NMR. Recrystallization from $C_3H_6O$ solution saturated by addition of ether gave after 1 month at −40 °C some red small needles used for the X-ray structure. This cation is very light sensitive, and all these operations were done in the dark: $^1H$ NMR ($C_3D_6O$, $Me_4Si$): δ 8.4–7.55 (m, 9 H, uncomplexed aromatic), 7.45–7.30, 6.6 (m, 3 H, complexed aromatic), 4.46 (s, 5 H, $C_5H_5$) ppm. $^{13}C$ NMR ($C_3D_6O$): δ 132.93, 132.07, 131.65, 130.73, 128.00, 127.76, 125.38, 125.25, 123.73 (uncomplexed CH), 135.25, 132.95, 130.76, 127.70, 121.62 (uncomplexed C), 87.76, 84.72, 80.15 (complexed CH), 96.27, 91.90, 91.59 (complexed C), 78.27 ($C_5H_5$). ESR data (77 K, frozen THF solution): $g = 2.0028$.

**6. [FeCp*(phenanthrene)]$^+PF_6^-$ (16).** $FeCp^*(CO)_2Br$ (3.27 g, 10 mmol), $AlCl_3$ (6.1 g, 45 mmol), and phenanthrene (3.6 g, 20 mmol) were stirred under argon in a round-bottom flask at 110 °C for 15 h. Workup proceeded as in section 1, giving 0.4 g (8% yield vs $FeCp^*(CO)_2Br$) of a yellow microcrystalline powder of **16**: $^1H$ NMR ($C_3D_6O$, $Me_4Si$): δ 8.3–7.4 (m, 6 H, uncomplexed aromatic), 6.1–6.8 (m, 4 H, complexed aromatic), 1.55 (s, 15 H, $C_5Me_5$) ppm. $^{13}C$ NMR ($C_3D_6O$): δ 134.7, 134.4 (uncomplexed C), 131–125.7 (uncomplexed CH), 95.11, 94.24 (complexed C), 91.7–82.5 (complexed CH), 8.8 ($CH_3$) ppm. Anal. Calcd for $C_{24}H_{25}FePF_6$: C, 56.03; H, 4.86. Found: C, 55.97; H, 4.79.

**7. [FeCp*(pyrene)]$^+PF_6^-$ (18).** $FeCp^*(CO)_2Br$ (1.5 g, 4.6 mmol), $AlCl_3$ (3.1 g, 23 mmol), and pyrene (1.9 g, 9.4 mmol) were stirred under argon in a round-bottom flask at 120 °C for 15 h. Workup proceeded as in section 1, giving 0.173 g (7% yield vs $FeCp^*(CO)_2Br$) of **18** as a yellow microcrystalline powder. $^1H$ NMR ($C_3D_6O$, $Me_4Si$): δ 8.76–8.1 (m, uncomplexed aromatic), 7–6.4 (m, 3 H, complexed aromatic), 1.36 (s, 15 H, $C_5Me_5$) ppm. $^{13}C$ NMR ($C_3D_6O$): δ 134.19, 130.57, 129.44, 127 (uncomplexed CH), 133.58, 126.8 (uncomplexed C), 94.27, 90 (complexed C), 90.13, 87.02 (complexed CH), 88.57 (C of $C_5Me_5$), 8.3 ($CH_3$) ppm. (The complexed region (two complexed CHs) confirms that complexation is of type B and not A (the latter would require only one type of complexed CH).) Anal. Calcd for $C_{26}H_{25}FePF_6$: C, 57.99; H, 4.64. Found: C, 57.77; H, 4.66. ESR data (77 K, frozen THF solution): $g_x = 2.0416$, $g_y = 2.0077$, $g_z = 1.9730$.

**8. [FeCp*(triphenylene)]$^+PF_6^-$ (17).** $FeCp^*(CO)_2Br$ (1.5 g, 4.6 mmol), $AlCl_3$ (3.1 g, 23 mmol), and triphenylene (1.4 g, 6 mmol) were stirred under argon in a round-bottom flask at 110 °C for 15 h. Workup proceeded as in section 1, giving 0.222 g (9% yield vs $FeCp^*(CO)_2Br$) of **17** as a yellow microcrystalline powder. $^1H$ NMR ($C_3D_6O$, $Me_4Si$): δ 8.86–8.26 (m, 4 H, uncomplexed aromatic), 7.93–7.63 (m, 4 H, uncomplexed aromatic), 7.33, 6.33 (m, 4 H, complexed aromatic), 1.3 (s, 15 H, $C_5Me_5$) ppm. $^{13}C$ NMR ($C_3D_6O$): δ 131.5, 129.69, 126.37, 125.19 (uncomplexed CH), 132.66, 127.32 (uncomplexed C), 91.26, 82.69 (complexed CH), 93.37 (complexed C), 91.12 (C of $C_5Me_5$), 8.7 ($CH_3$) ppm. Anal. Calcd for $C_{28}H_{27}FePF_6$: C, 59.57; H, 4.78. Found: C, 59.70; H, 4.82.

**9. [FeCp*(biphenyl)]$^+PF_6^-$ (12).** $FeCp^*(CO)_2Br$ (6.5 g, 20 mmol), $AlCl_3$ (13.5 g, 100 mmol), and biphenyl (0.8 g, 5 mmol) were mixed under argon and heated at 90 °C in 100 mL of Decalin for 15 h. Workup proceeded as in section 1, giving 2.28 g (90% yield vs biphenyl) of **12** as a yellow microcrystalline powder. $^1H$ NMR ($C_3D_6O$, $Me_4Si$): δ 8.03, 7.56 (m, 5 H, uncomplexed aromatic), 6.63, 6.16 (m, 5 H, complexed aromatic), 1.76 (s, 15 H, $C_5Me_5$) ppm. $^{13}C$ NMR ($C_3D_6O$): δ 132.76 (uncomplexed C), 131.14, 130.30, 128.05 (uncomplexed CH), 101.49 (complexed C), 90.97, 90.79, 85.34 (complexed C), 91.86 (C of $C_5Me_5$), 9.52 ($CH_3$) ppm. Anal. Calcd for $C_{22}H_{25}FePF_6$: C, 53.87; H, 5.10. Found: C, 54.05; H, 5.24.

**10. Generation of Fe(I) and Monoreduced Complexes.** The

**Table V. Positional Parameters (×10⁴) of Non-Hydrogen Atoms for [CpFe(perylene)]$^+PF_6^-$**

| atom | x | y | z |
|---|---|---|---|
| | Molecule A | | |
| Fe(30) | 1507 (3) | 4665 (2) | 6798 (3) |
| P(40) | 4844 (6) | 3126 (6) | 4364 (6) |
| F(41) | 5249 (16) | 3727 (19) | 3234 (17) |
| F(42) | 3605 (13) | 3310 (12) | 4406 (17) |
| F(43) | 4795 (18) | 2190 (16) | 4162 (23) |
| F(44) | 4852 (20) | 4099 (17) | 4597 (25) |
| F(45) | 6062 (11) | 2983 (13) | 4319 (13) |
| F(46) | 4438 (19) | 2569 (24) | 5432 (15) |
| C(1) | 1446 (15) | 5153 (14) | 8071 (16) |
| C(2) | 1141 (19) | 6052 (15) | 8308 (16) |
| C(3) | −0027 (20) | 6245 (14) | 8842 (17) |
| C(4) | −0826 (19) | 5503 (18) | 9145 (15) |
| C(5) | −0506 (18) | 4565 (16) | 8901 (15) |
| C(6) | 0672 (16) | 4435 (15) | 8359 (15) |
| C(7) | 2585 (21) | 4963 (14) | 7511 (18) |
| C(8) | 2918 (18) | 4059 (17) | 7264 (19) |
| C(9) | 2159 (19) | 3376 (18) | 7485 (17) |
| C(10) | 1026 (20) | 3485 (15) | 8100 (16) |
| C(11) | 0187 (23) | 2719 (15) | 8408 (15) |
| C(12) | −0954 (23) | 2886 (19) | 8960 (18) |
| C(13) | −1248 (22) | 3825 (15) | 9159 (17) |
| C(14) | −1939 (21) | 5587 (18) | 9650 (18) |
| C(15) | −2302 (22) | 6514 (22) | 9885 (20) |
| C(16) | −1587 (19) | 7240 (18) | 9682 (17) |
| C(17) | −0376 (22) | 7149 (15) | 9102 (16) |
| C(18) | 0455 (19) | 7847 (17) | 8838 (18) |
| C(19) | 1584 (22) | 7667 (17) | 8328 (17) |
| C(20) | 1934 (18) | 6742 (15) | 8054 (17) |
| C(31) | 0432 (24) | 5653 (21) | 6209 (20) |
| C(32) | 0393 (22) | 4669 (22) | 6096 (18) |
| C(33) | 1485 (21) | 4446 (17) | 5550 (17) |
| C(34) | 2266 (23) | 5205 (17) | 5262 (18) |
| C(35) | 1606 (28) | 5973 (19) | 5670 (21) |
| | Molecule B | | |
| Fe(90) | −3109 (3) | 0929 (2) | 7292 (3) |
| P(80) | −2607 (6) | −0072 (5) | 10819 (5) |
| F(81) | −2654 (28) | 0967 (18) | 10412 (26) |
| F(82) | −3523 (20) | −0221 (23) | 10498 (17) |
| F(83) | −3377 (19) | −0046 (26) | 11814 (17) |
| F(84) | −1693 (19) | 0171 (16) | 11166 (14) |
| F(85) | −1845 (22) | −0061 (25) | 9812 (15) |
| F(86) | −2450 (29) | −1071 (14) | 11309 (22) |
| C(51) | −1520 (16) | 0285 (14) | 6739 (15) |
| C(52) | −0430 (18) | 0719 (12) | 6429 (15) |
| C(53) | 0104 (17) | 1256 (14) | 5382 (15) |
| C(54) | −0465 (16) | 1335 (12) | 4644 (16) |
| C(55) | −1613 (17) | 0958 (13) | 4978 (17) |
| C(56) | −2095 (17) | 0384 (13) | 6032 (15) |
| C(57) | −2044 (20) | −0217 (16) | 7789 (17) |
| C(58) | −3146 (21) | −0534 (16) | 8099 (18) |
| C(59) | −3738 (21) | −0376 (18) | 7407 (21) |
| C(60) | −3193 (18) | 0023 (14) | 6364 (18) |
| C(61) | −3750 (20) | 0152 (17) | 5654 (23) |
| C(62) | −3233 (21) | 0632 (17) | 4649 (21) |
| C(63) | −2141 (20) | 1012 (15) | 4320 (18) |
| C(64) | 0103 (19) | 1827 (15) | 3620 (15) |
| C(65) | 1171 (17) | 2191 (14) | 3276 (15) |
| C(66) | 1693 (18) | 2112 (15) | 3961 (16) |
| C(67) | 1183 (16) | 1623 (15) | 4989 (16) |
| C(68) | 1732 (19) | 1493 (15) | 5697 (19) |
| C(69) | 1251 (20) | 1011 (16) | 6730 (19) |
| C(70) | 0152 (22) | 0616 (20) | 7116 (19) |
| C(91) | −3615 (17) | 2330 (16) | 6619 (21) |
| C(92) | −4450 (24) | 1803 (20) | 7419 (25) |
| C(93) | −4134 (23) | 1591 (17) | 8307 (21) |
| C(94) | −2701 (20) | 2404 (16) | 6868 (21) |
| C(95) | −3008 (25) | 1900 (19) | 7986 (26) |
| | Diethyl Ether | | |
| C(201) | −4841 (26) | 3423 (23) | 10138 (24) |
| O(202) | −3929 (18) | 3955 (15) | 9274 (16) |
| C(203) | −4057 (26) | 4539 (23) | 8260 (24) |
| C(204) | −2991 (29) | 4969 (25) | 7641 (27) |
| C(205) | −4567 (31) | 2984 (27) | 11042 (28) |

**Table VI. Extended Hückel Parameters**

| orbital | | | exponents[a] | |
|---|---|---|---|---|
| | | $H_{ii}$, eV | $\zeta_1$ | $\zeta_2$ |
| H | 1s | -13.60 | 1.30 | |
| C | 2s | -21.40 | 1.625 | |
| | 2p | -11.40 | 1.625 | |
| Fe | 4s | -9.10 | 1.90 | |
| | 4p | -5.32 | 1.90 | |
| | 3d | -12.60 | 5.35 (0.5366) | 1.80 (0.6678) |

[a] Two Slater exponents are listed for the 3d functions. Each is followed in parentheses by the coefficient in the double-$\zeta$ expansion.

complex $[FeCp(arene)]^+PF_6^-$ and $LiAlH_4$ (25 mol/mol of Fe complex) were mixed under argon and placed in a ESR tube at -80 °C. Then THF was added by canula at -90 °C, and the reaction mixture was allowed to warm up slightly under argon. When a strong color change from pale yellow (suspension) to the deep color of the soluble radical species was observed, the mixture was cooled down again to 77 K. These solutions were used for ESR measurements.

**11. X-ray Crystallography.** A crystal of dimensions 0.1 × 0.2 × 0.4 mm was mounted on a Nonius CAD 4 diffractometer. Lattice parameters were determined from least-squares adjustment setting angles of 25 reflections with $8 \leq 2\theta \leq 19°$. The space group is triclinic, space group $P\bar{1}$, with a unit cell of dimensions $a$ = 12.803 (4) Å, $b$ = 14.225 (9) Å, $c$ = 14.727 (6) Å, $\alpha$ = 72.53 (3)°, $\beta$ = 69.26 (3)°, and $\gamma$ = 83.13 (5)°. The observed volume of 2392 Å$^3$ is consistent with two independent molecules in the asymmetric unit. A total of 4370 independent reflections were collected by using a graphite-monochromated Mo K$\alpha$ radiation and the following experimental conditions: $0.5 \leq \theta \leq 21°$; scan type $\omega/\theta$; scan angle $\Delta\theta = (1.50 + 0.35 \tan \theta)°$; detector aperture $D$ (mm) = 2.0 + 0.5 tan $\theta$. A total of 2041 unique reflections having $I \geq 1\sigma(I)$ (poor quality of crystal and hence of intensity data) were considered as observed. The data corrected from $L$ and $P$ factors were used in the structure determination. The structure was solved by direct methods (MITHRIL).[45]

Hydrogen atoms were located from difference Fourier syntheses along with an included diethyl ether molecule.

Due to the very high thermal parameters of the ether molecule, it was not possible to find other hydrogen atoms. The last least-squares refinement including anisotropic thermal parameters for all non-hydrogen atoms converged to $R = \sum[|F_o| - |F_c|]/\sum|F_o| = 0.094$. The hydrogen parameters were not refined, and their temperature factors were set equal to $B_{eq}$ of their carrier atoms. Positional parameters of non-hydrogen atoms are reported in Table V.

**Acknowledgment.** We are grateful to M. Petraud and B. Barbe (CESAMO, University of Bordeaux) for diligent NMR assistance, to the "Laboratoire de Chimie du Solide" (Bordeaux) for kindly recording ESR spectra, to J. G. Melin for skillful experimental assistance, and to F. Leroy for his helpful assistance in the X-ray study.

## Appendix

**(a) EH Calculations.** All the calculations have been carried out within the extended Hückel formalism[41] using the weighted $H_{ij}$ formula.[42] The utilized atomic parameters are summarized in Table VI. The following bond lengths (Å) and bond angles (deg) have been used: Fe–C = 2.10; C(Cp)–C(Cp) = 1.42; C(arene)–C(arene) = 1.40; C–H = 1.09; C–C–C(Cp) = 108°; C–C–C(arene) = 120°.

**Table VII. SCF-MS-X$\alpha$ Parameters**

| atomic sphere | radius, au | $\alpha$ |
|---|---|---|
| Fe | 2.2795 | 0.711 51 |
| C | 1.6535 | 0.753 81 |
| H | 0.8758 | 0.777 25 |
| E[a] Cp | 1.0843 | 0.762 90[c] |
| E[a] arene | 1.3226 | 0.762 90[c] |
| out.[b] benzene | 6.4246 | 0.762 90[c] |
| out.[b] naphthalene | 10.3133 | 0.762 60[c] |
| out.[b] pyrene | 10.3133 | 0.761 89[c] |

[a] Empty sphere. [b] Outer sphere. [c] Weighted average of atomic values.

**(b) SCF-MS-X$\alpha$ Calculations.** The standard version of the method was used.[43] Starting from the geometry-induced touching spheres, the carbon radii were enlarged by 25% to assume a better description of the ring systems[44] and an additional empty sphere has been located in the center of each ring. This procedure resulted in the muffin-tin radii given in Table VII. The atomic exchange parameter $\alpha$ was obtained from Schwartz tabulation,[45] except for hydrogen where the Slater value[46] was chosen. Those relative to the extramolecular (outer-sphere) and inner-sphere regions are weighted-average values of the atomic ones.

Potential waves up to $l = 2$ are included in the multiple scattering expansions in the metal sphere and the extramolecular regions; up to $l = 1$ in the carbon and empty spheres. Only the $l = 0$ value was considered for hydrogen spheres. SCF calculations were converged to better than ±0.0001 Ry on each level.

For the three studied complexes, the calculations have been carried out by using a perfect $C_s$ symmetry with planar and parallel ligands in which the C–C and C–H bond distances are respectively 1.40 and 1.10 Å. For CpFe(benzene) the Fe–ligand distances are those observed in $CpFe(C_6Me_6)$:[28a] Fe–Cp = 1.78 Å and Fe–benzene = 1.54 Å. In the naphthalene and pyrene complexes the Fe–arene distance is kept at 1.54 Å. Two calculations have been carried out for CpFe(naphthalene): one with an Fe–Cp distance of 1.78 Å and the other one with a distance of 1.70 Å (see text). The Fe–Cp distance used for CpFe(pyrene) is 1.70 Å.

**Registry No.** **1**, 12176-31-7; **2**, 38117-78-1; **3**, 59236-70-3; **4**, 69039-93-6; **5**, 59183-95-8; **6**, 69005-60-3; **7**, 113287-99-3; **8**, 70755-99-6; **9**, 89031-71-0; **10**, 67734-82-1; **11**, 76747-93-8; **12**, 113288-01-0; **13**, 88760-61-6; **15**, 108917-11-9; **16**, 113288-03-2; **17**, 113288-05-4; **18**, 113316-18-0; $FeCp^*(CO)_2Br$, 34808-38-3; CpFe(benzene), 51812-05-6; CpFe(naphthalene), 51812-06-7; CpFe(phenanthrene), 69022-31-7; CpFe(triphenylene), 121072-57-9; CpFe(pyrene) (isomer A), 121055-72-9; CpFe(pyrene) (isomer B), 121072-58-0; CpFe(perylene), 121055-73-0; CpFe(coronene), 121055-74-1; ferrocene, 102-54-5; phenanthrene, 85-01-8; pyrene, 129-00-0; triphenylene, 217-59-4; coronene, 191-07-1; perylene, 198-55-0; biphenyl, 92-52-4.

**Supplementary Material Available:** Tables of hydrogen positional parameters and anisotropic thermal parameters of non-hydrogen atoms (2 pages); a listing of structure factors (27 pages). Ordering information is given on any current masthead page.

(41) (a) Hoffmann, R. *J. Chem. Phys.* **1963**, *39*, 1397. (b) Hoffmann, R.; Lipscomb, W. N. *J. Chem. Phys.* **1962**, *36*, 2179; **1962**, *37*, 2872.
(42) Ammeter, J. H.; Bürgi, H. B.; Thibeault, J. C.; Hoffmann, R. *J. Am. Chem. Soc.* **1978**, *100*, 3686.
(43) (a) Slater, J. C. *Adv. Quantum Chem.* **1972**, *6*, 1. (b) Johnson, K. H. *Ibid.* **1973**, *7*, 143.
(44) Herman, F.; Williams, A. R.; Johnson, K. H. *J. Chem. Phys.* **1974**, *61*, 3508.
(45) (a) Schwarz, K. *Phys. Rev.* **1972**, *B5*, 2466. (b) Slater, J. C. *Int. J. Quantum Chem.* **1973**, *75*, 533.
(46) Gilmore, C. J. *J. Appl. Cryst.* **1984**, *17*, 42.